Volume 23, No 4 | International Journal of Radiation Research, October 2025

Development and *in-vitro* evaluation of gallium-68 labelled Staphylococcus aureus -specific aptamer as a potential PET agent for infection imaging

S. Bargh[1], C. Ozkul[2], S.S. Timur[3], V.C. Ozalp[4], S. Erdogan[1*]

[1]Department of Radiopharmacy, Faculty of Pharmacy, Hacettepe University, Ankara, Turkiye
[2]Department of Pharmaceutical Microbiology, Faculty of Pharmacy, Hacettepe University, Ankara, Turkiye
[3]Department of Pharmaceutical Technology, Faculty of Pharmacy, Hacettepe University, Ankara, Turkiye
[4]Department of Biology, Faculty of Medicine, Atılım University, Ankara, Turkiye

► ***Original article***

Corresponding author:
Suna Erdogan, Ph.D.,
E-mail:
serdogan@hacettepe.edu.tr

Received: September 2024
Final revised: January 2025
Accepted: February 2025

Int. J. Radiat. Res., October 2025; 23(4): 1037-1042

DOI: 10.61186/ijrr.23.4.29

Keywords: *Aptamer, gallium-68, Staphylococcus aureus, PET agent for infection imaging.*

ABSTRACT

Background: Staphylococcus aureus (S. aureus) is the most common causative pathogen associated with a wide range of infections, from mild to life-threatening conditions such as osteomyelitis, endocarditis, and pneumonia. Early detection and reliable differentiation between infection and sterile inflammation are essential for accurate diagnosis and effective treatment. However, most radiopharmaceuticals currently available fail to discriminate between these conditions, underscoring the need for infection-specific imaging agents. ***Materials and Methods:*** In this study, a Gallium-68 (Ga-68)-labeled S. aureus-specific aptamer was developed as a potential PET infection imaging probe. Aptamers were selected using the cell- systematic evolution of ligands by exponential enrichment (SELEX) method, and their specificity was verified by fluorescence-based binding assays. Radiolabeling was achieved via DOTA chelation, and radiochemical purity was determined. Additionally, in vitro binding assays were performed with S. aureus, while Escherichia coli (E. coli) served as a control. ***Results:*** The aptamer exhibited an affinity constant (K_a) of 2260 ± 634 CFU/mL and a linear detection range of 250-2×10^4 CFU/mL, with a limit of detection of 171 CFU/mL for S. aureus. The Ga-68-labeled aptamer demonstrated radiochemical purity greater than 99%. In vitro binding increased linearly with rising S. aureus concentrations (10^3-2×10^4 CFU/mL), while minimal binding to E. coli confirmed its specificity. ***Conclusion:*** These results demonstrate that the Ga-68-labeled S. aureus-specific aptamer holds promise as an infection-targeted PET imaging agent. Although currently limited to in vitro evaluation, such aptamer-based radiopharmaceuticals may contribute to improved diagnosis and imaging of infectious diseases.

INTRODUCTION

Staphylococcus aureus (S. aureus) is among the most common causative agents of human infections. It is frequently implicated in a wide spectrum of diseases, from mild skin and soft tissue infections to severe, life-threatening conditions, and is therefore of great medical importance [1]. The diagnosis of infection typically begins with clinical suspicion based on symptoms and basic laboratory tests, including C-reactive protein (CRP) levels and erythrocyte sedimentation rate (ESR). Radiography is often the initial imaging modality; however, plain radiographic findings may be unremarkable, particularly in the early stages of the disease. Therefore, confirmation typically requires blood tests, cultures, biopsies, or advanced imaging techniques. Magnetic resonance imaging (MRI) and radionuclide imaging methods have significantly improved diagnostic accuracy and the ability to characterize infections [2].

Radionuclide imaging enables early diagnosis by detecting increased activity within 24–48 hours after the onset of symptoms. Moreover, hybrid imaging modalities such as Positron Emission Tomography/ Computed Tomography (PET/CT), Single Photon Emission Computed Tomography (SPECT)/CT, and PET/MRI provide superior performance by evaluating both structural and pathophysiological processes, thereby enhancing specificity and diagnostic accuracy [3]. A variety radiopharmaceutical labeled with gallium-67 (Ga-67), technetium-99m (Tc -99m), indium-111 (In-111), iodine-131 (I-131), and fluorine-18 (F-18) have been developed for infection imaging [4, 5]. However, most radiopharmaceuticals currently used in SPECT and PET infection imaging are inadequate for distinguishing infection from sterile inflammation [6]. Consequently, there remains a critical need to develop novel infection-specific radiopharmaceuticals.

Aptamers have emerged as highly promising affinity tools in biosensor development and

[DOI: 10.61186/ijrr.23.4.29]

molecular imaging because of their ability to bind target molecules with high specificity. Radiolabeled aptamers have been explored as diagnostic probe across various imaging modalities, enhancing the visualization of biological targets as diagnostic tracers. The majority of radionuclide imaging studies employing aptamers have been directed toward oncological applications. In contrast, their use in infection imaging remains markedly underexplored, with only a limited number of reports available, predominantly involving *S. aureus*–specific aptamers have been radiolabeled with Tc-99m and investigated for their potential in infection detection [7-9]. Nevertheless, PET imaging is well recognized for its substantially higher sensitivity compared to other imaging modalities [10], enabling high-resolution imaging even at low radiotracer concentrations [11].

Among PET radionuclides, Ga-68 offers several advantages that make it particularly attractive for aptamers labeling. These include its short half-life, which enables rapid imaging, as well as its commercial availability, accessibility, and improved bioconjugation yields [12]. Collectively, these features improve imaging quality and diagnostic accuracy, making Ga-68-labeled aptamers particularly valuable for applications requiring high specificity and rapid results.

This study was design to develop and evaluate a Ga-68-labeled *S. aureus*-specific aptamer as a promising PET imaging probe for the detection of infections. To the best of our knowledge, the preparation, quality control, and evaluation of the specificity for *S. aureus* of a Ga-68–labeled aptamer has not been reported until now.

MATERIALS AND METHODS

Bacterial strains and culture

Frozen cultures of *S. aureus* (ATCC 43000, USA) and *E. coli* (ATCC 25922, USA), used as control bacteria, were inoculated onto Tryptic Soy Agar (TSA) (Sigma-Aldrich, Germany) and incubated overnight at 37°C. Bacterial growth was monitored by measuring turbidity at 600 nm with NanoDrop Microvolume Spectrophotometer (Thermo Fisher Science, USA), and bacteria in the logarithmic growth phase were collected for subsequent experiments.

Aptamer selection (Cell-SELEX)

Aptamers were selected using a method similar to the cell-SELEX procedure described in a previous study [13]. Briefly, a DNA SELEX library (10.4 nmol) (sequence: GGCGGCGATGAGGATGAC-N38-ACCACT GCGTGACTGCC) (Sigma-Aldrich, Germany) was incubated with 2×10^5 S. aureus cells in 1× PBS (phosphate-buffered saline) (Merck, Germany) for 30 min. The suspension was washed three times with PBS, centrifuged, and the bacterial pellt containing bound ssDNA sequences was eluted and amplified by PCR (Polymerase Chain Reaction) (Bio-Rad, USA). PCR amplification was performed under the following conditions: initial denaturation at 95 °C for 3 min, followed by 10 cycles of 95 °C for 30 s, 55 °C for 30 s, and 72 °C for 30 s, with a final extension at 72 °C for 5 min. The molecular weight of the PCR products was verified by gel electrophoresis (Bio-Rad, USA) after each cycle.

The resulting double-stranded PCR products were subsequently converted into ssDNA using biotin-labeled reverse primers (Sigma-Aldrich, Germany). For this purposes, the double-stranded PCR products were incubated with streptavidin-coated magnetic beads (Sigma-Aldrich, Germany) in PBS for one hour. Non-biotinylated ssDNA strands were then separated by heating at 95 °C for 5 min and collected to form the ssDNA library for the next SELEX cycle. To enhance specificity, bovine serum albumin (BSA, 1 mg/mL; Merck, Germany) was employed for counter-selection, eliminating non-specific binders, while Listeria monocytogenes was used for negative selection to further refine specificity.

The final library members obtained after the last SELEX round were sequenced using next-generation sequencing (NGS) (Illumina, USA) according to previously established protocols [14]. Briefly, PCR amplicons from the final SELEX cycle were generated using the forward and reverse SELEX primers (Part #15044223 Rev. B, Illumina, Inc., California, USA) and their size was confirmed by 4% (w/v) agarose gel electrophoresis. Dual-index sequences were incorporated into the amplicons using the Nextera XT Index Kit v2 Set-A (Illumina, USA) and purified with AMPure XP beads (Beckman Coulter, USA). The DNA library was diluted to 35 pM, and a 5% (v/v) PhiX control v3 (Illumina, USA) was added as a control DNA sample. A total of 20 µL of the prepared library, including PhiX DNA, was loaded into the iSeq 100 i1 cartridge (300 cycles), and sequencing was performed on the iSeq 100 system (Illumina, USA) using paired-end reads. MEME Suite stream analysis was subsequently applied to identify common sequence motifs and categorize sequences into distinct groups [15].

Assessment of aptamer binding to S. aureus

Fluorescein-labeled aptamers were employed to evaluate the binding affinity of the selected aptamers (table 1) for *S. aureus*. The bacterial concentration was set at 10^7 cells/mL, and aptamer concentrations ranged from 100 pM to 2 µM. After 30 minutes of incubation at room temperature, bound library members were isolated by washing and elution via centrifugation. Fluorescence measurements were recorded at 480 nm excitation and 520 nm emission using a plate reader (FLUOstar Omega; BMG Labtech, Germany), and binding values were subsequently calculated. Each aptamer was tested in triplicate, and

[DOI: 10.61186/ijrr.23.4.29]

the fluorescence signal (aptamer binding rate) measured at different aptamer concentrations was analysed using a single-subtraction equation (equation 1). The binding constant was determined according to equation 2.

$$Binding = \frac{Bound\ aptamer\ fluorescence\ value}{Initial\ total\ fluorescence\ value} \times 100 \quad (1)$$

$$Y = \frac{(B_{max} \times [X])}{(K_d + [X])} \quad (2)$$

Y = fluorescent signal (RFU)
B_{max} = Maximum specific binding
X = aptamer concentration (µM)
K_d = affinity constant

Visualization of aptamer binding to S. aureus by fluorescence microscopy

The binding specificity of the aptamer was assessed in *S. aureus* and *E. coli* (negative control) using fluorescence microscopy. For this analysis, *S. aureus* and *E. coli* were resuspended in PBS at a concentration of 10^7 CFU/mL (Colony Forming Unit/ mL) and incubated for 45 minutes with FAM (fluorescein amidite)–labeled aptamers (5′ labeling). The bacterial–aptamer complexes were washed three times with PBS and examined using a Leica DMIL inverted microscope (Leica, Germany) [16].

Biocompatibility of aptamers

The aptamers' biocompatibility was evaluated *in vitro* using the L929 mouse fibroblast cell line (ATCC, USA). Cells were cultured in RPMI 1640 medium supplemented with 4 mM L-glutamine, sodium pyruvate, 10% fetal bovine serum (FBS), and 1% penicillin-streptomycin (10,000 U/10,000 µg/mL) under standard incubation conditions (5% CO_2 at 37 °C).

For the assay, cells were seeded into 96-well plates at a density of 5×10^4 cells/mL and incubated overnight. The following day, cells were treated with the aptamer at concentrations ranging from 0.1 µM to 10 µM. After 24 hours of incubation, cell viability was assessed using the MTT assay. Briefly, MTT reagent (3-(4,5-dimethylthiazol-2-yl)-2,5-diphenyltetrazolium bromide; Sigma Aldrich, Germany) was added to each well at a final concentration of 1 mg/mL, and cells were incubated for 4 hours. Following incubation, the medium was removed, and the resulting formazan crystals were dissolved in DMSO (Dimethyl sulfoxide; Sigma-Aldrich, Germany). Optical density (OD) was measured at 570 nm using an ELISA microplate reader (Molecular Devices, Silicon Valley, CA, USA) [17]. The biocompatibility of the aptamer–DOTA conjugate employed in radiolabeling studies was similarly evaluated using the same methodology.

Synthesis of aptamer-DOTA conjugate

For radiolabeling studies, the 5′-amine-functionalized aptamer was conjugated with DOTA-NHS ester (1,4,7,10-tetraazacyclododecane-1,4,7,10-tetraacetic acid mono-N-hydroxysuccinimide ester; Macrocyclics, USA). Bioconjugation was performed following a previously described method [18]. Briefly, the aptamer was dissolved in 0.1 M sodium bicarbonate (Merck, Germany) (pH 8) to a final concentration of 100 µM, while DOTA was dissolved in DMSO at 20 mM. The reagents were incubated at room temperature for 2 hours under continuous shaking [18]. The resulting conjugate was purified using a NAP 25 column (Merck, USA), lyophilized, and stored at 4 °C. Aptamer-DOTA conjugation was confirmed using matrix-assisted laser desorption/ ionization time-of-flight mass spectrometry (MALDI-TOF, Bruker Daltonics, Germany).

Radiolabeling of aptamers with Ga-68

For radiolabeling, Ga-68 was eluted from the Ge-68/Ga-68 generator (Eckert & Ziegler, Germany), and 300 µL of the aptamer-DOTA conjugate, dissolved in 1 M HEPES (4-(2-hydroxyethyl)-1-piperazineethanesulfonic acid; Sigma-Aldrich, Germany) buffer (pH 5), was mixed with 100 µL of Ga -68 solution (approximately 50 µCi). The mixture was incubated for 15 minutes at 90 °C [6, 19].

Radiochemical purity was assessed using instant thin-layer chromatography (ITLC-SG) plates (Sigma-Aldrich, Germany) as the stationary phase and ammonium acetate/methanol (1 M, 50/50) as the mobile phase. The samples were analyzed using a radio-TLC scanner (Eckert & Ziegler, Germany).

The in vitro stability of the Ga-68-labeled aptamer complex was evaluated in saline at room temperature and in plasma at 37 °C. Aliquots were collected at 0, 15-, 30-, 60-, and 120-minutes post-incubation and analyzed by TLC as described above [6, 19].

In vitro binding assay of Ga-68 labeled aptamer to S. aureus

The Ga-68-labeled aptamer was incubated with varying concentrations of bacterial cells at a dose of 50 µCi for 30 minutes at 37 °C. Following incubation, the aptamer-incubated bacterial suspensions were centrifuged at 13,000 rpm for 10 minutes. The supernatant was discarded, and the pellets were washed three times with PBS (pH 7.4). The resulting bacterial pellets were resuspended in 200 µL of PBS (pH 7.4), and their radioactivity was measured using a gamma counter. The same procedure was performed using *E. coli* as a negative control [7].

RESULTS

Aptamer selection and assessment of aptamer binding to S. aureus

S. aureus-specific aptamers were selected using the SELEX procedure. Following the thirteenth SELEX cycle, a twofold increase in the number of bound

[DOI: 10.61186/ijrr.23.4.29]

library members was observed. A total of 46,659 sequences were identified during this cycle. These sequences were classified into distinct motif groups based on common 6–7 base-long motifs identified through motif-search analysis. The most abundant motif groups included 16,380 sequences containing the GGACC motif (aptamer-1), 15,509 sequences containing the AGTCA motif (aptamer-2), 3,986 sequences containing the ATCGACC motif (aptamer-3), and 2,174 sequences containing the ACTGG motif (aptamer-4) (table 1). The four most prevalent motifs represented 35%, 33%, 8%, and 5% of the sequences, respectively.

In the pool binding assay, selected aptamer candidates were synthesized with 5′-fluorescent labeling and tested for target and nontarget binding. Aptamer-1 and Aptamer-2 exhibited 63% and 59% binding, while Aptamer-3 and Aptamer-4 showed 34% and 21% binding, respectively. Binding of the nontarget mixture (*E. coli* and BSA) to Aptamer-1 and Aptamer-2 was 26% and 39%, respectively. The binding data indicated that Aptamer-1 had the highest affinity for *S. aureus* with relatively low binding to *E. coli*, and this sequence was therefore selected for further experiments.

The binding of aptamer to varying concentrations of *S. aureus* followed the one-substrate Langmuir equation (figure 1). The affinity constant (K_D) for Aptamer-1 was calculated as 2260 ± 634 CFU/mL, with a linear range of 250-2×10^4. The limit of detection (LOD) for *S. aureus* was determined to be 171 CFU/mL using the 3σ method.

Visualization of aptamer binding to S. aureus by fluorescence microscopy

To confirm the specificity of Aptamer-1 for *S. aureus*, fluorescence microscopy was used to visualize aptamer binding to *S. aureus* and *E. coli* (control bacteria). Bacterial cells were incubated with FAM-labeled aptamers and examined under a fluorescence microscope. Aptamer-1 was observed to bind to *S. aureus* (figure 2). *E.coli* was used as the control bacteria and no detectable fluorescence signal was observed in these bacteria.

Biocompatibility of aptamer

The biocompatibility of the aptamer was evaluated *in vitro* using the L929 mouse fibroblast cell line. Changes in cell viability were expressed as a percentage relative to control cells. As shown in figure 3, cell viability decreased as the concentrations of the aptamer and the aptamer-DOTA conjugate increased after 24 hours of incubation. Although the aptamer-DOTA conjugate exhibited slightly higher toxicity than the aptamer alone, a comparative analysis of cell viability at different concentrations (0.1, 0.5, 1, 5, and 10 µM) revealed no statistically significant difference between the aptamer and the aptamer-DOTA conjugate after 24 hours ($p > 0.05$).

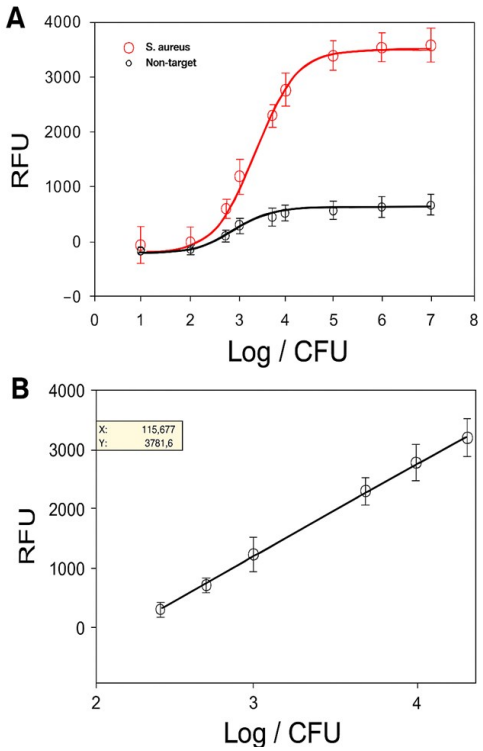

Figure 1. Fluorescence signal as a function of bacterial cell concentration. **(A)** Binding specificity of the aptamer towards Staphylococcus aureus (red) compared to non-target bacteria (black). **(B)** Linear correlation between fluorescence intensity and bacterial cell concentration within the dynamic detection range. RFU indicates relative fluorescence units, and CFU denotes colony-forming units.

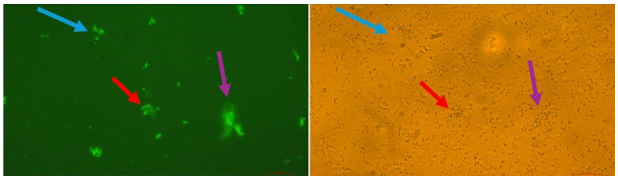

Figure 2. Fluorescence **(A)** and light **(B)** microscopy images of aptamer binds to Staphylococcus aureus. Fluorescence microscopy showing aptamer binding to S. aureus (indicated by arrows). Corresponding light microscopy image of the same sample, confirming bacterial cell morphology. Scale bar: 0.1 µm.

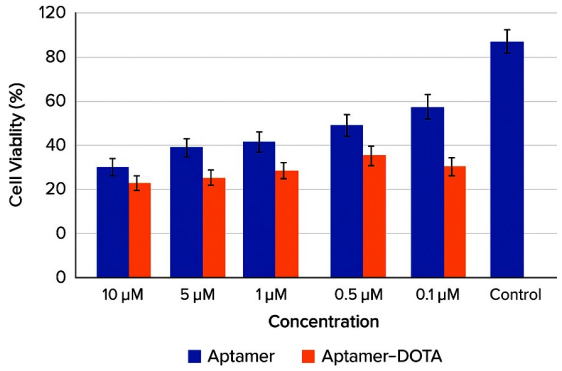

Figure 3. Cell viability following incubation with aptamers and aptamer–DOTA conjugates. L929 cells were incubated with different concentrations (10, 5, 1, 0.5, and 0.1 µM) of aptamer or aptamer–DOTA for 24 h. Cell viability (%) was expressed relative to untreated control cells. Data are presented as mean ± SEM (n = 5).

[DOI: 10.61186/ijrr.23.4.29]

Synthesis of aptamer-DOTA conjugate and radiolabeling with Ga-68

The 5′-amine-functionalized aptamer was successfully conjugated with DOTA-NHS ester, and the formation of the aptamer-DOTA conjugate was confirmed using MALDI-TOF mass spectrometry. Mass spectrometry analysis verified the successful conjugation of the chelator to the aptamer by detecting the expected increase in molecular weight following the reaction. As anticipated, the average molecular weight of the conjugated aptamer was 13,337 Dalton, confirming the covalent attachment of the chelator to the aptamer (figure 4).

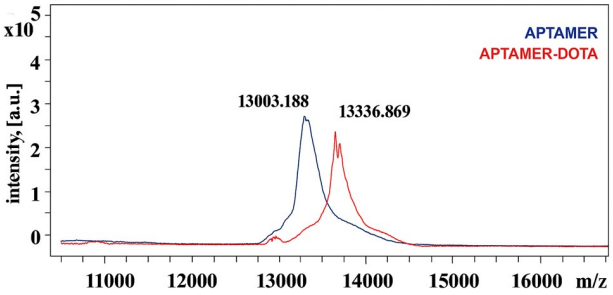

Figure 4. MALDI-TOF mass spectrometry analysis confirming aptamer–DOTA conjugation. The mass spectrum of the unmodified aptamer (blue) shows a major peak at m/z 13,003, whereas the aptamer–DOTA conjugate (red) displays a shifted peak at m/z 13,336, consistent with the expected mass increase after DOTA conjugation.

After bioconjugation, the DOTA-conjugated aptamers were successfully labeled with Ga-68, achieving high radiochemical yield and purity (>99%) (figure 5). The radiolabeled aptamer demonstrated high stability (~99%) for up to 60 minutes in both saline and plasma at room temperature and at 37°C.

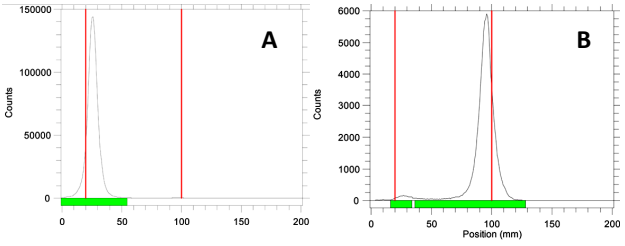

Figure 5. Radiolabeling of DOTA-conjugated aptamers with gallium-68. **(A)** Chromatographic profile of Ga-68 eluate following anionic purification, showing a sharp peak corresponding to free Ga-68. **(B)** Chromatographic profile of the Ga-68-DOTA-aptamer complex, demonstrating a shift in peak position, consistent with successful radiolabeling.

In vitro binding assay of Ga-68 labeled aptamer to S. aureus

To confirm that the aptamer retained its specificity and continued to bind *S. aureus* after radioactive labeling, an *in vitro* binding assay was performed using the Ga-68-labeled *S. aureus*-specific aptamer. Following incubation of the Ga-68-labeled aptamer with *S. aureus*, the amount of bound aptamer was quantified by measuring the radioactivity signal, which exhibited a linear increase with rising bacterial concentrations from 1×10^3 to 2×10^4 CFU (R^2 = 0.99). This result confirms that Ga-68-labeled aptamer probe successfully identifies the *S. aureus*, target bacteria. Moreover, the low-level radioactivity observed in the presence of *E. coli* (control bacteria), further supports the specificity of the aptamer (figure 6).

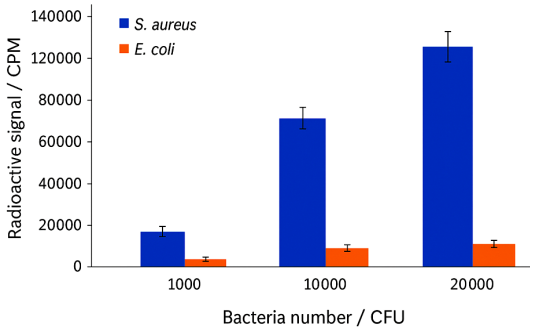

Figure 6. Binding assay of Ga-68–labeled aptamers to S. aureus and E. coli (control). Radioactive signal (CPM) increased proportionally with the number of S. aureus cells, while minimal binding was observed to E. coli. Data are presented as mean ± SEM (n = 3).

DISCUSSION

Bacterial infections represent a significant global health challenge due to their high morbidity, mortality, and the increasing prevalence of antimicrobial resistance. Affinity targeting with radiopharmaceuticals provides an effective strategy to overcome many of the limitations associated with conventional infection imaging. Aptamers are a relatively novel class of molecules in radiopharmaceutical research, and their application in infection imaging remains underexplored [20].

In our study, we successfully selected an *S. aureus* –specific aptamer through iterative SELEX cycles, and Aptamer-1 was identified as the most promising candidate based on its high binding affinity and relatively low non-specific binding to *E. coli*. The binding parameters obtained (K_D = 2260 ± 634 CFU/mL, LOD = 171 CFU/mL) are comparable to those reported in previous aptamer-based infection imaging studies [21], supporting the potential of our aptamer as a highly sensitive molecular probe. Fluorescence microscopy images further confirmed the specificity of Aptamer-1, as clear binding was observed to *S. aureus* but not to *E. coli*, reinforcing its diagnostic value.

Aptamers, being synthetic DNA or RNA molecules, do not elicit an immune response like natural proteins (e.g., antibodies). Therefore, they are highly biocompatible and are often considered advantageous compared to antibodies, to which they share certain similarities [22]. The literature also reports that in studies involving drug delivery systems and nanoparticles, surface modification with

[DOI: 10.61186/ijrr.23.4.29]

aptamers enhances their biocompatibility [23, 24]. Our results demonstrate a favorable biocompatibility profile for both the aptamer and its DOTA-conjugated form. The lack of significant cytotoxicity in L929 fibroblasts indicates that these aptamer conjugates are well tolerated, a critical prerequisite for their potential use in future in vivo applications.

Furthermore, the aptamer was efficiently radiolabeled with Ga-68, yielding high radiochemical purity (>99%) and stability in both saline and plasma, which are critical attributes for any radiopharmaceutical intended for PET imaging [19].

The *in vitro* binding assays with the Ga-68-labeled aptamer demonstrated preserved target specificity after radiolabeling, with a strong linear correlation between bacterial load and radioactivity signal (R^2 = 0.99). Minimal binding to *E. coli* further highlights the selectivity of the probe.

CONCLUSION

Collectively, our findings provide a strong proof-of-concept that Ga-68 labeled aptamer-based radiopharmaceuticals can be developed for PET infection imaging. In vitro binding studies confirmed that the Ga-68-labeled aptamer retained high affinity and specificity for *S. aureus*, further supporting its potential as an infection-targeted PET probe. Although limited to *in vitro* evaluation, the observed binding specificity, stability, and biocompatibility underscore the promise of Ga-68-labeled aptamers and highlight the need for further in vivo studies to validate their diagnostic utility and potential clinical translation.

***Acknowledgment*:** The authors gratefully acknowledge the support provided by the TÜBİTAK project No. 221S418.

***Conflicts of interests*:** This work was supported by the Scientific and Technological Research Council of Turkiye (TÜBİTAK) under Project No. 221S418.

***Funding*:** Nothing to declare.

***Ethical considerations*:** This study did not involve human or animal subjects; ethical approval was not required.

Author contributions: SB: Investigation, experimentation, data collection, writing, reviewing, and editing. COK: Supervision and methodology. SST: Supervision and methodology VCO: Writing - original draft, supervision. SE: Conceptualization, funding acquisition, supervision, writing, reviewing, and editing.

REFERENCES

1. dos Santos AL, Santos DO, de Freitas CC, Alves Ferreira BL, Afonso IF, Rodrigues CR, Castro HC (2007) *Staphylococcus aureus*: visitando uma cepa de importância hospitalar. *J Bras Patol Med Lab*, ***43*** *:413-23*.
2. Hatzenbuehler J and Pulling TJ (2011) Diagnosis and management of osteomyelitis. *Am Fam Physician*, ***84****(9): 1027-33*.
3. Navalkissoor S, Nowosinska E, Gnanasegaran G, Buscombe JR (2013) Single-photon emission computed tomography–computed tomography in imaging infection. *Nucl Med Commun*, ***34****(4): 283-90*.
4. Patel RD, Patel PM, Patel NM (2011) A review on radiopharmaceuticals and radiochemical method in analysis. *Int J Pharm Biol Arch*, ***2****: 1062-7*.
5. Salmanoglu E, Kim S, Thakur ML (2018) Currently available radiopharmaceuticals for imaging infection and the holy grail. *Semin Nucl Med*, ***48****(2): 86-99*.
6. Mokoala KM, Ndlovu H, Lawal I, Sathekge MM (2024) PET/CT and SPECT/CT for infection in joints and bones: an overview and future directions. *Semin Nucl Med*, ***54****(3): 394-408.*
7. dos Santos SR, Corrêa CR, de Barros AL, Serakides R, Fernandes SO, Cardoso VN, *et al.* (2015) Identification of *Staphylococcus aureus* infection by aptamers directly radiolabeled with technetium -99m. *Nucl Med Biol*, ***42****(3): 292-8*.
8. Ferreira IM, de Sousa Lacerda CM, dos Santos SR, de Barros ALB, Fernandes SO, Cardoso VN, *et al.* (2017) Detection of bacterial infection by a technetium-99m-labeled peptidoglycan aptamer. *Biomed Pharmacother*, ***93****: 931-8*.
9. Correa CR, Miranda AS, Simionatto CS, Lima WM, Souto AA, Silva RG, *et al.* (2014) Aptamers directly radiolabeled with technetium-99m as a potential agent capable of identifying carcinoembryonic antigen in tumor cells T84. *Bioorg Med Chem Lett*, ***24****(8): 1998-2001.*
10. Termaat MF, Raijmakers PG, Scholten HJ, Bakker FC, Patka P, Haarman HJ (2005) The accuracy of diagnostic imaging for the assessment of chronic osteomyelitis: a systematic review and meta -analysis. *J Bone Joint Surg Am*, ***87****(11): 2464-71*.
11. Smith DL, Breeman WA, Sims-Mourtada J (2013) The untapped potential of gallium-68 PET: the next wave of 68Ga agents. *Appl Radiat Isot*, ***76****: 14-23*.
12. Vanbrocklin HF. Radiochemistry of PET. In: Schwaiger M, Reske SN, editors. *Molecular Imaging: Principles and Practice*. New York: McGraw-Hill; 2010. p. 304.
13. Dursun AD, Borsa BA, Bayramoglu G, Arica MY, Ozalp VC (2022) Surface plasmon resonance aptasensor for *Brucella*detection in milk. *Talanta*, ***239****: 123074*.
14. Ersoy Omeroglu E, Sudagidan M, Yurt MN, Tasbasi BB, Acar EE, Ozalp VC (2021) Microbial community of soda Lake Van as obtained from direct and enriched water, sediment and fish samples. *Sci Rep*, **11**(1): 18364.
15. Bailey TL, Boden M, Buske FA, Frith M, Grant CE, Clementi L, *et al.* (2009) MEME SUITE: tools for motif discovery and searching. *Nucleic Acids Res*, **37**: W202-8.
16. Farrel Côrtes M, Bes T, Deo BR, Barbosa dos Anjos B, Jimenez Galisteo AJ Jr, Cerdeira Sabino E, *et al.* (2022) Selection and identification of a DNA aptamer for multidrug-resistant *Acinetobacter baumannii* using an in-house cell-SELEX methodology. *Front Cell Infect Microbiol*, ***12****: 818737*.
17. Timur SS (2023) Anticancer potential of novel nanoemulgel formulations in melanoma. *FABAD J Pharm Sci*, ***48****(3): 443-58*.
18. Sicco E, Báez J, Margenat J, García F, Ibarra M, Cabral P, *et al.* (2018) Derivatizations of Sgc8-c aptamer to prepare metallic radiopharmaceuticals as imaging diagnostic agents: Syntheses, isolations, and physicochemical characterizations. *Chem Biol Drug Des*, ***91****(3): 747-55.*
19. Tayeri H, Sattarzadeh Khameneh E, Zolghadri S, Kakaei S, Sardari D (2020) Optimized production, quality control and biological assessment of 68Ga-bleomycin as a possible PET imaging agent. *Int J Radiat Res*, ***18****(2): 235-41*.
20. Liu X, Zhao Y, Wang X, Wu L, Zhang Y, Lu W, *et al.* (2025) Preclinical evaluation of 68Ga-labeled SL1 aptamer for c-Met targeted PET imaging. *Mol Pharm*, ***22****(3): 1615-23*.
21. Kolm C, Cervenka I, Aschl UJ, Baumann N, Jakwerth S, Krska R, *et al.* (2020) DNA aptamers against bacterial cells can be efficiently selected by a SELEX process using state-of-the-art qPCR and ultra-deep sequencing. *Sci Rep*, ***10****(1): 20917*.
22. Jayasena SD (1999) Aptamers: an emerging class of molecules that rival antibodies in diagnostics. *Clin Chem*, ***45****(9): 1628-50*.
23. Thelu HVP, Siriki A, Devanathan P, Kaloor SH, Shajesh V, Reji V (2019) Self-assembly of an aptamer-decorated, DNA-protein hybrid nanogel: a biocompatible nanocarrier for targeted cancer therapy. *ACS Appl Bio Mater*, ***2****(12): 5227-34*.
24. Foster A and DeRosa MC (2014) Development of a biocompatible layer-by-layer film system using aptamer technology for smart material applications. *Polymers (Basel)*, ***6****(5): 1631-44.*

[DOI: 10.61186/ijrr.23.4.29]